Proceedings of International Conference on Technology and Social Science 2017
Invited Paper

Electric Field Signal Simulation from Fixed Transmitter in Intra-body Communication

Keisuke Furuya [1,a], Yuki Wada [1], Ryota Kato[1], Yutaro Toyoshima[1], Mitsuru Shinagawa[1], Ken Seo[2], Daisuke Saito[2], Kyoji Oohashi[2], and Yuichi Kado[3]

[1]Faculty of Science and Engineering, Hosei University, 3-7-2, Kajino-cho, Koganei-shi, Tokyo, 184-8584, Japan

[2]Nippon Signal CO., LTD, 11-2, Hiraide-Kogyo-Danchi, Utsunomiya-shi, Tochigi, 321-8651, Japan

[3]Department of Electronics, Kyoto Institute of Technology, Matsugasaki, Sakyo-ku, Kyoto, 606-8585, Japan

[a]< keisuke.furuya.7s@stu.hosei.ac.jp >

Keywords: intra-body communication, unintentional path communication, wearable transmitter, fixed transmitter

Abstract. The electromagnetic field simulation of an electric field signal from an alternating current (AC) driven transmitter is described. As the ground node of an AC driven transmitter is strongly coupled to the earth ground, we think that the correct path signal and unintentional path signal of the AC driven transmitter are larger than those of a battery driven transmitter. We examined the correct-to-unintentional path signal ratio (*CUR*) by means of an electromagnetic field simulation and found that the *CUR* of a fixed transmitter is almost equal to that of a wearable transmitter.

1. Introduction

Intra-body communication [1, 2] has been investigated for improving the usability of Internet of Things (IoT) services. Intra-body communication uses the human body as a communication path [3], so a natural action such as stepping on a floor mat is a communication trigger [4, 5]. A correct path occurs between the hot electrodes of two communication devices. However, there can also be an unintentional path signal between the hot and cold electrodes of two communication devices. The ground node of an AC driven transmitter is strongly coupled to the earth ground, and we know that the unintentional path signal of the fixed transmitter is larger than that of the wearable transmitter. The *CUR* of the fixed transmitter and wearable transmitter should be investigated precisely by means of an electromagnetic field simulation.

2. Unintentional path communication

Figure 1 shows the communication path models of a wearable transmitter driven by a battery: (a) correct path and (b) unintentional path. The signal from the hot electrode of a wearable transmitter WT1 propagates to the hot electrode of a fixed receiver FR1.The communication path is defined as a correct path signal. The voltage between the hot and cold electrodes of the FR1 is V_{cf}. The signal from the cold electrode of the wearable transmitter WT2 propagates to the hot electrode of the FR1. The communication path is defined as an unintentional path signal. The voltage between the hot and cold electrodes of the FR1 is V_{uf}. The correct-to-unintentional path signal ratio of the wearable transmitter CUR_W is written as

$$CUR_W = 20 \times \log_{10} (V_{cf}/V_{uf}). \quad (1)$$

The communication path models of a fixed transmitter driven by an AC power: (a) correct path and (b) unintentional path are shown in Fig. 2. The signal from the hot electrode of a fixed transmitter FT1 propagates to the hot electrode of a wearable receiver WR1. The communication path is defined as the correct path signal. The voltage between the hot and cold electrodes of the WR1 is V_{cw}. A signal from the hot electrode of the FT1 propagates to the cold electrode of a wearable receiver WR2. The communication path is defined as an unintentional path signal. The voltage between the hot and cold electrodes of the WR2 is V_{uw}. The correct-to-unintentional path signal ratio of the fixed transmitter CUR_{F} is written as

$$CUR_{\mathrm{F}} = 20 \times \log_{10}(V_{\mathrm{cw}}/V_{\mathrm{uw}}). \quad (2)$$

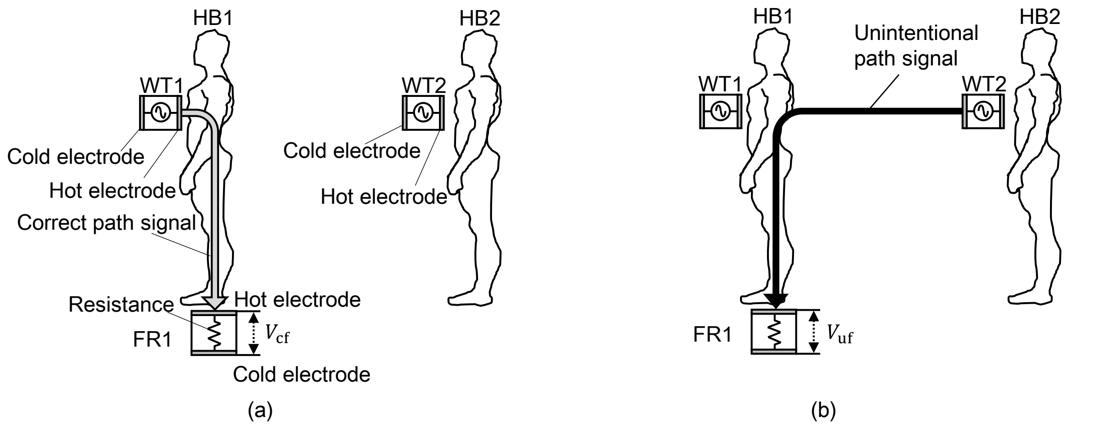

Fig. 1. Communication path models of wearable transmitter driven by battery: (a) correct path and (b) unintentional path.

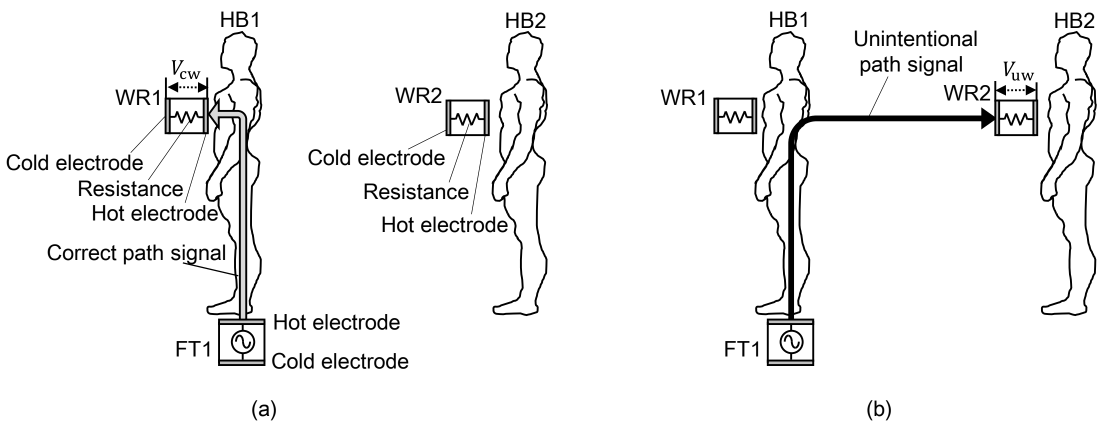

Fig. 2. Communication path models of fixed transmitter driven by AC power: (a) correct path and (b) unintentional path.

3. Electromagnetic field simulation model

Figure 3 shows the configurations of the (a) electromagnetic field simulation model, (b) wearable device, and (c) fixed device. The electromagnetic field simulation was performed using EMPro (Keysight Technologies). The human bodies HB1 and HB2 wear the wearable devices. The HB1 stands on the fixed device. The distance between the HB1 and HB2 is *D*. The electromagnetic property of the human body is assigned as a muscle. The conductivity and relative permittivity of the muscle are 0.602 S/m and 234, respectively [6]. When a communication device works in a transmitting mode, the device is an ideal transmitter with the internal impedance of 0 Ω. The output sinusoidal signal amplitude is 1 $V_{0\text{-}p}$ and the frequency is 6.75 MHz. When a communication device works in a receiving mode, the input impedance is 1 MΩ between the hot and cold electrodes of the receiver. The hot and cold electrodes of the wearable device and the fixed device are 1 mm thick and material is Cu. The wearable devices consist of an acrylonitrile butadiene styrene (ABS) resin case and the hot and cold electrodes. The distance between the human body and the wearable device is 5 mm. The relative permittivity of the ABS resin is 2.8. The fixed device consists of three formed styrol plates and the hot and cold electrodes. The conductivity and relative permittivity of the foamed styrol are 1.0×10^{-15} S/m and 1.03. The cold electrode of the fixed device is electrically connected to the Cu ground through a pillar of Cu.

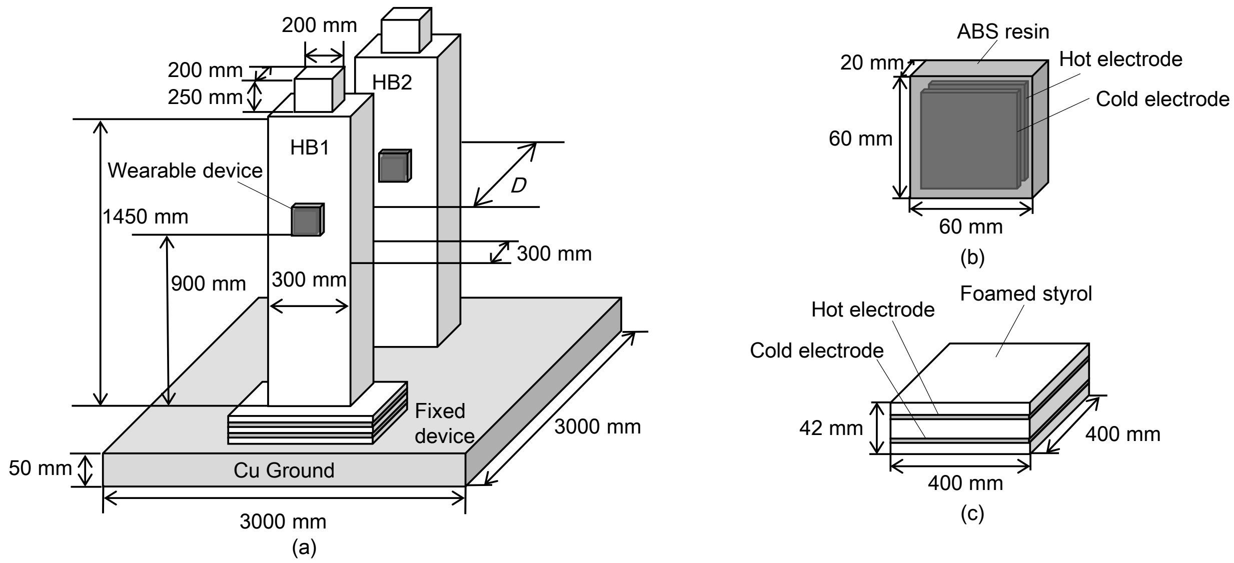

Fig. 3. Configurations of (a) electromagnetic field simulation model, (b) wearable device and (c) fixed device.

4. Simulation results

The *CUR* of a wearable transmitter or fixed transmitter was simulated by changing the *D* from 400 mm to 1000 mm. The *D* dependence of (a) the received signal amplitude and (b) the *CUR* are shown in Fig. 4. The unintentional path signal decreases by extending the *D*. The correct path signal amplitude and unintentional path signal amplitude of the fixed transmitter were significantly larger than those of the wearable transmitter, as we had suspected they would be. We also found that the CUR_F was nearly equal to the CUR_W. We thought that the transmission characteristics of the communication path models of the wearable transmitter driven by a battery (Fig. 1) were nearly equal to those of the communication path models of the fixed transmitter driven by AC power (Fig. 2).

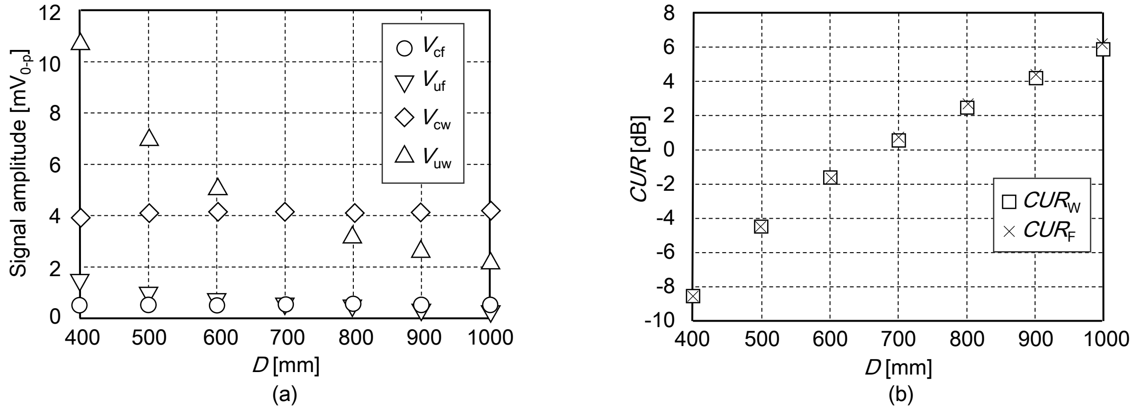

Fig. 4. Distance *D* dependence of (a) received signal amplitude and (b) correct-to-unintentional path signal ratio.

5. Conclusion

The electric field signal from a fixed transmitter in intra-body communication was investigated by means of electric field simulation. Results showed that the correct path signal and unintentional path signal of the fixed transmitter were larger than those of the wearable transmitter. The CUR_W and CUR_F were almost the same when the same simulation model was used. These results demonstrate that the *CUR* is independent of the drive type of the transmitter when the transmission characteristics are the same.

References

[1] T. G. Zimmerman, "Personal Area Networks: Near-field Intrabody Communication," ***IBM System Journal***, vol. 35, no. 3-4, pp. 609-617, 1996.

[2] N. Haga, K. Motojima, M. Shinagawa, and Y. Kado, "Equivalent-Circuit Expression of Environmental Noise Electric Fields in Intrabody Communication Channels," ***IEEE Transactions on Electromagnetic Compatibility***, vol. 58, no. 1, pp. 294-306, 2016.

[3] K. Matsumoto, J. Katsuyama, R. Sugiyama, Y. Takizawa, S. Ishii, M. Shinagawa, and Y. Kado, "Signal Measurement System for Intra-body Communication Using Optical Isolation Method," ***OPTICAL REVIEW***, vol. 21, no. 5, 2014.

[4] S. Hasegawa, M. Ishida, I. Yokota, Y. Kado, K. Ohashi, D. Saito, "Human Body Equivalent Phantom for Analyzing of Surface and Space Propagation in MHz-Band Signal Transmission," ***Antennas and Propagation*** (EuCAP), 2016.

[5] Y. Hayashida, M. Hasegawa, A. Suzuki, M. Shinagawa, Y. Kado, and N. Haga, "Radiated Noise Analysis via Human Body for Intra-body Communication," ***Measurement Elsevier***, vol. 89, pp. 159-165, 2016.

[6] G. Camelia, "Compilation of The Dielectric Properties of Body Tissues at RF and Microwave Frequencies," pp. 26-27, 1996.